Electropolymerization of Aniline Over Chemically Converted Graphene-Systematic Study and Effect of Dopant

Hagar K. Hassan, Nada F. Atta, Ahmed Galal[*]

Department of Chemistry, Faculty of Science, Cairo University, 12613 Giza, Egypt
Tel.:+20 0235676561, Fax: +20 0235727556
[*]E-mail: galal@sci.cu.edu.eg

Graphene was chemically prepared using microwave irradiation. Aniline was electropolymerized over graphene immobilized on glassy carbon substrate potentiostatically in a three-electrode-one compartment cell. A systematic study of chemically converted graphene/PANI composites in both monomer free solution and potassium ferricyanide/ferrocyanide redox system was performed. The resulted chemically converted graphene/poly(aniline) (CCG/PANI) composite was characterized using surface techniques such as field emission scanning electron microscope (FE-SEM) and atomic force microscope (AFM). The effect of different dopants on the electrochemical behavior of CCG/PANI in several protonic acids was also investigated. The diffusion coefficients of proton and counterion (anion) as well as the average diffusion coefficients in these protonic acids were calculated. The results revealed that the presence of graphene enhances the electrochemical performance of PANI in both monomer free solution and potassium ferricyanide. A synergetic electrocatalytic effect resulted when combining PANI and CCG as manifested by a noticeable increase in current signals.

1. INTRODUCTION

Polyaniline (PANI) is one of the conducting polymers which attracts a great attention due to its low cost, ease of synthesis [1], having good environmental stability, reversible redox activity, and potential applications in sensing, energy conversion and storages [2–10]. Due to its facile preparation, high conductivity and good environmental stability [11], polyaniline (PANI) is a popular material for coatings having porous structures for various applications [12, 13]. One of PANI's most interesting features is its ability to be electrochemically switched between electronically insulating and conducting states, during which hydrogen ions are incorporated into or expelled from the polymer phase [14]. The

chemistry of PANI was studied on different surfaces by several researchers such as the direct electropolymerization of PANI on bare GCE [12,13]. Several researchers studied the electropolymerization of PANI on the surface of carbon nanotubes (CNTs) [15-17]. And there are other publications that indicated the use of PANI/CNTs composites in many applications, this composite was prepared by one step synthesis [18].

Graphene was considered as the missing allotrope of pure carbon materials, after the discovery of graphite, diamond, fullerenes and carbon nanotube [19]. Graphene is a member of 2-dimentional materials discovered by Andre Geim's research group at the University of Manchester in 2004, and prepared by the so-called "scotch-tape" technique [20]. Graphene is a one atom thick structure that consists of a hexagonal array of Sp^2- bonded carbon [21-24] atoms and looks like a honey comb [21, 25, 26]. It can be considered as the mother of all carbon materials where, SWCNTs can be viewed as the result of rolling up a sheet of graphene [27, 28]. On the other hand, graphite is one of the oldest known carbon allotropes and can be considered as a stacked graphene sheets while graphene can be coalesced to form fullerene [29].

Graphene has some unique properties which make it one of the most interesting materials nowadays even compared to CNTs. The optical and electrical properties of reduced graphene oxide depend on the spatial distribution of the functional groups and structural defects [30]. Some of its properties are: has large theoretical surface area about 2620 m^2/g [25, 28, 31], chemically stable and almost impermeable to gases, can withstand large current densities, has high thermal [19] and chemical conductivity [32, 33] including extremely high charge (electrons and holes) mobility (230,000 cm^2/Vs) with 2.3% absorption of visible light [34, 35] and thermal conductivity (3000 W/mK), has outstanding mechanical properties [33, 36], the highest strength (130 GPa), has large amount of edge planes/defects [32], and is less expensive to produce compared to CNTs [33].

The discovery of graphene and graphene-based polymer nanocomposites is an important addition in the area of nanoscience and plays a key role in modern science and technology [37]. In the past several years, there has been a growing interest in the preparation, structural characterization and applications of graphene/conduction polymer (CP) composites [38–50]. This is mainly due to the fact that there are several complementary properties between CPs and graphene, especially those related to electrochemical activity, conductivity and mechanical strength. It is expected that the hybridization of CPs with graphene would be attractive for combining the properties of both components or improving the properties of the resulting composites based on the resulting synergetic effects. Thus, graphene/CP nanocomposites show superior mechanical, thermal, gas barrier, electrical and flame retardant properties compared to the neat polymer [37, 51–58].

Graphene/PANI composites can be prepared either by electrochemical polymerization of aniline monomer on the prepared graphene sheets [2] or in situ intercalative polymerization where, graphene oxide/PANI composites were firstly prepared by the oxidation of aniline in graphene oxide (GO) dispersion. Then, the obtained composites were reduced by treating it with hydrazine, giving the CCG/PANI composites [3, 4, 10]. PANI can combine with GO to form GO/PANI composites. The possible modes of combination in GO/PANI are proposed as follows: (a) π-π stacking (b) electrostatic interactions, and (c) hydrogen bonding [59].

To the best of our knowledge there is no previous work that introduced a systematic study of PANI grown on the surface of CCG. The aim of this work is to study the electrochemical behavior of CCG/PANI systematically including the optimization and the characterization of the electropolymerized PANI on glassy carbon/chemically converted graphene (GC/CCG) surface as well as studying the doping/undoping processes of PANI on the surface of GC/CCG in presence of several protonic acids.

2. EXPERIMENTAL

2.1. Materials and Chemicals

All chemicals were used as received without further purification except for aniline that was purified by distillation. Graphite powder, sulfuric acid, nitric acid, hydrochloric acid, orthophosphoric acid, potassium ferricyanide, dimethylformamide (DMF) and hydrazine hydrate (HH) were supplied by Aldrich Chem. Co. (Milwaukee, WI. USA).

2.2. Preparation of chemically converted graphene (CCG)

Initially graphene oxide (GO) was prepared by oxidation of spectroscopic grade graphite powder using the method of Hummers [60]. The following summarizes the protocol followed: 1 g of graphite powder (spectroscopic grade) and 0.525 g of sodium nitrate into 24 ml of 93% H_2SO_4 were vigorously stirred. The ingredients were mixed and cooled to 0^oC in an ice-bath and 5.0 g of potassium permanganate was added to the suspension. The ice-bath was then removed and the temperature of the suspension is brought to 35 ± 3^oC, where it was maintained for 90 minutes then water (48 ml) was slowly stirred into the paste. The diluted suspension (brown in color) was maintained at this temperature for 15 minutes. The suspension was then further diluted to approximately 150 ml with warm water and treated with 30% hydrogen peroxide that turned it into bright yellow suspension. Graphene oxide was filtrated and washed several times and left to dry.

Chemically converted graphene was prepared by chemical reduction of graphene oxide (GO) using microwave irradiation in the presence of hydrazine hydrate (HH) as a reducing agent [61]. Thus, 0.1 g of GO was sonicated with 20 ml of deionized water until a homogeneous yellow dispersion was obtained. Graphene oxide can be dispersed easily in water due to the presence of a variety of hydrophilic oxygen groups (OH, O, COOH). After adding 150 µl of HH, the solution was placed in a conventional microwave oven (MC-9283 JLR, 900 W) and operated at a full power 900 W in 30 s cycles (on for 10 s, off and stirring for 20 s) for a total reaction time of 120 sec.

After microwave irradiation the yellow color of the solution was converted into black that indicates the complete reduction of GO into CCG. The graphene flakes were separated by Mark IV auto bench centrifuge operated at 5000 rpm for 15 minutes and dried overnight.

2.3. Electrochemical cells and equipments

Electrochemical experiments were carried out in a three-electrode/one-compartment glass cell. The working electrode was a GC electrode (diameter: 3 mm), reference electrode was Ag/AgCl (4.0 M KCl) and a Pt wire (5 cm long; diameter: 2 mm) as auxiliary electrode. GC electrode was polished using alumina (<2 µm)/water slurry) until no scratches were observed. About 10 µl of CCG suspension was added onto the surface of GC electrode. GC/CCG was left to dry at 70 ^{o}C, and then GC/CCG was subjected for aniline electropolymerization. The polymerization bath consists of 0.1 M aniline monomer dissolved in 0.5 M different supporting electrolytes (H_3PO_4, HCl, HNO_3 or H_2SO_4). Aniline was polymerized at constant potential (+800 mV to +1100 mV) for (20 s to 120 s).

The electrochemical characterizations were performed using BAS-100B electrochemical analyzer (Bioanalytical systems, BAS, West Lafayette, USA) that was connected to a personal computer. All experiments were carried out at temperature 25 ± 0.2 ^{o}C.

2.4. Structural and surface characterization

X-ray diffraction (XRD) was recorded on Panlytical X`Pert using Cu-Kα radiation (λ = 1.540 Ẵ). Surface measurements were achieved using field-emission scanning electron microscope (FE-SEM) by a JEOL JSM7000F Field Emission Scanning Electron Microscope and the atomic force microscope (AFM) by Shimadzu Wet – SPM (Scanning Probe microscope). AFM roughness data were used to calculate the real surface area according to the following relation:

$$\text{Surface roughness} = \frac{\text{Real surface area}}{\text{Geometric surface are}} \tag{1}$$

In this respect, the "real" surface area for GC/CCG and GC/CCG/PANI was calculated from the surface roughness as indicated in equation (1).

3. RESULTS AND DISCUSSION

3.1 Surface characterization

Figure (1) shows the XRD of graphite, GO and CCG. The XRD of CCG shows no peak neither around 11-12 Å as in case of GO nor around 26 Å as in case of graphite this indicates the successful preparation of CCG from the reduction of GO.

The field-emission scanning electron microscope images in Figures (2A), (2B and 2D), and (2C and 2E) for GC/CCG, GC/PANI, and GC/ CCG/PANI, respectively, with different magnifications are shown. It is shown that the chemically converted graphene sheets are rippled and crumpled with a dimension of several nm to few µm.
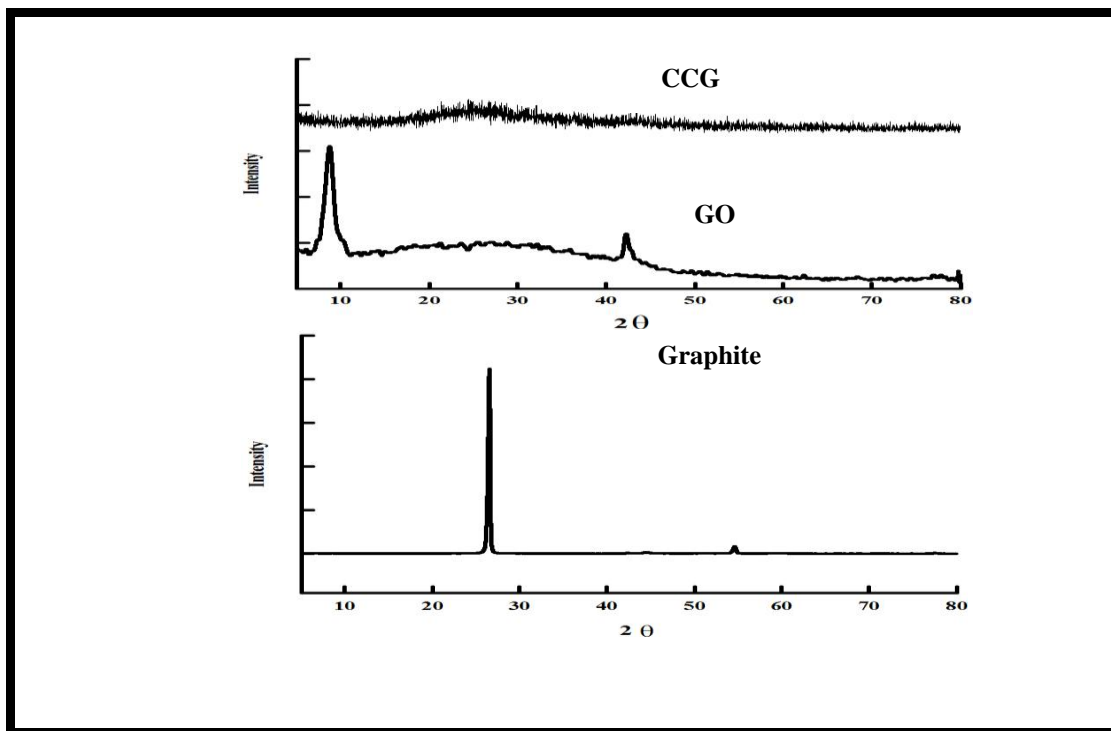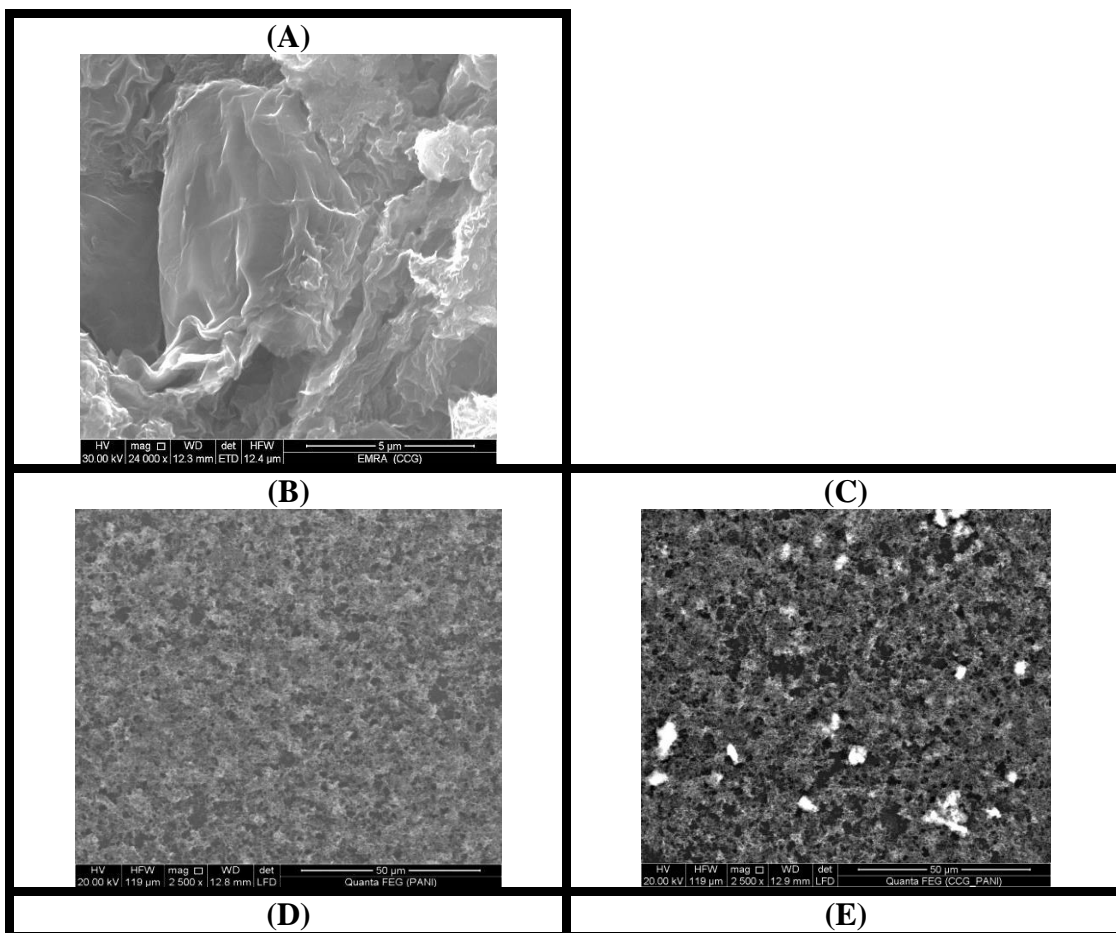
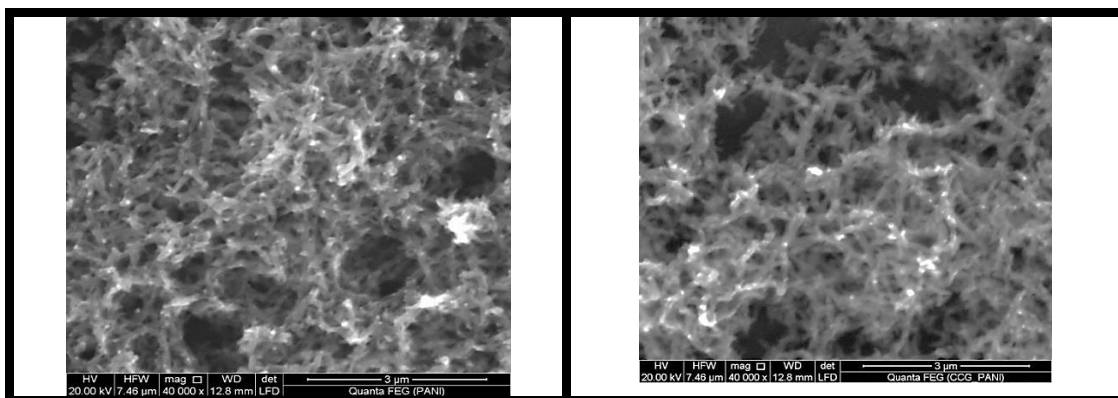**Figure 1.** The XRD of graphite, GO and CCG

Figure 2. A) FE-SEM of CCG, **B)** and **D)** FE-SEM of GC/PANI with magnification 2500 and 40000, respectively, **C)** and **E)** CG/CCG/PANI with magnification 2500 and 40000, respectively.
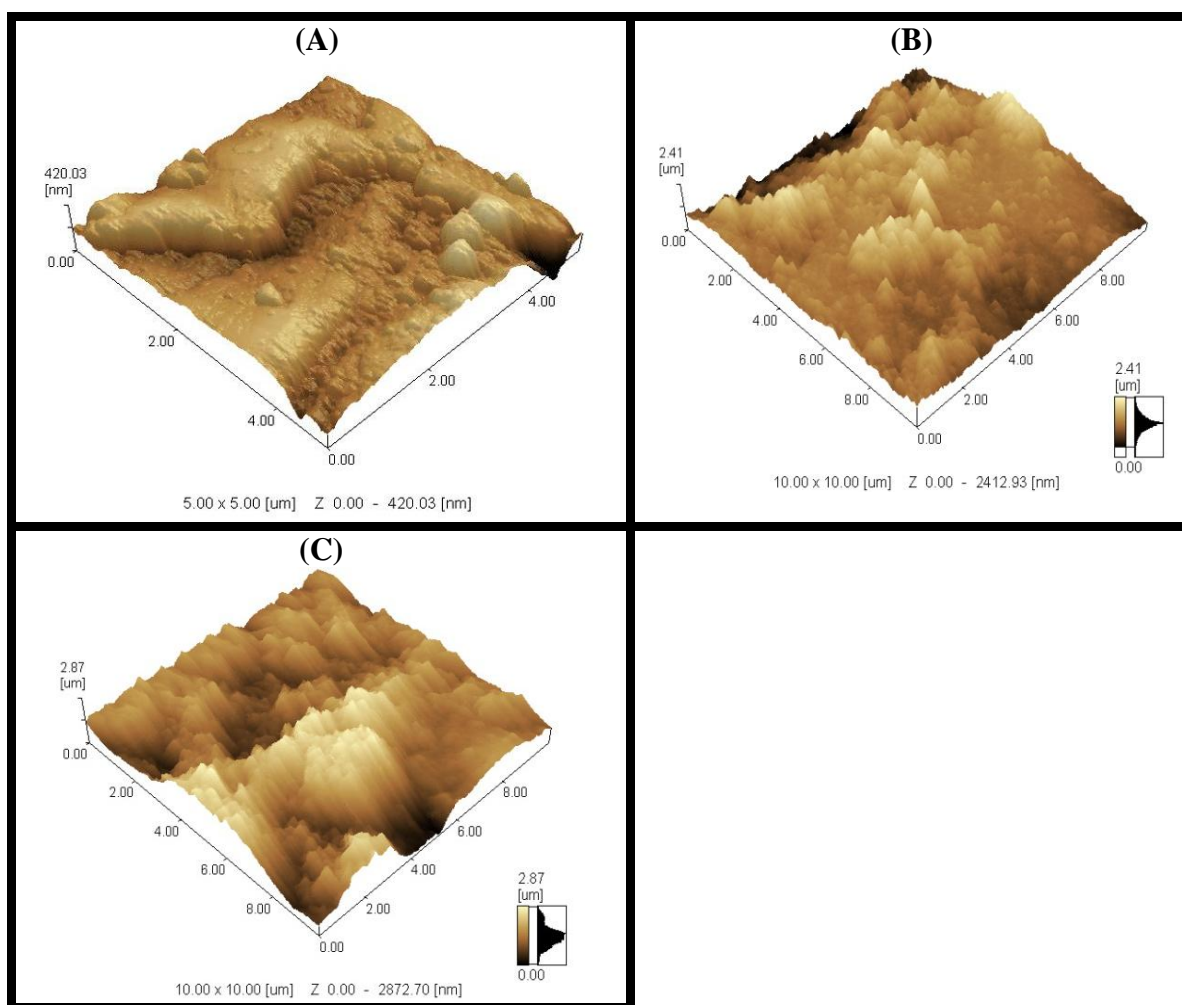

Figure 3. 3-dimensional AFM of **A)** GC/CCG, **B)** GC/PANI and **C)** GC/CCG/PANI.

PANI was deposited as fibers on both surfaces (GC and CCG) and reveal to be more compact and have relatively smaller diameter in absence of CCG. On the other hand, the porosity of PANI films

increases in the presence of CCG. This result indicates that the use of CCG as a solid substrate affects the morphology of the electropolymerized PANI film.

The three dimensional AFM images of GC/CCG (A), GC/PANI (B) and GC/CCG/PANI (C) are shown in Figure (3). As clearly seen from the AFM images, the GC/CCG/PANI shows more curves and humps compared to GC/PANI. This indicates that the presence of graphene increases the surface roughness and consequently the real surface area. The calculated surface roughness and real surface area for GC/CCG, GC/PANI and GC/CCG/PANI are 1.67, 1.3623, 1.502 and 0.118 cm^2, 0.0962 cm^2 and 0.106 cm^2, respectively

3.2.2. Electrochemical behavior of graphene/polyaniline (CCG/PANI) composite in monomer free solution

Cyclic voltammograms of PANI deposited on bare GC electrode in 0.5 M H$_2$SO$_4$ is characterized by three pairs of current peaks (three peaks in the anodic direction and three in the cathodic one) [62]. These peaks are due to doping and undoping of protons and anions in PANI film [62] and the transformation between different forms of PANI [63].

The oxidation peak around +200 mV is attributed to the conversion from leucoemeraldine into emeraldine form, the second peak appearing around +800 mV is due to emeraldine/pernigraniline transformation [62-65] and the current peak around +500 mV is assigned to the formation of benzoquinone (BQ) as side product due to overoxidation or degradation of PANI film [63]. BQ can be produced through two consecutive reactions involving the hydrolysis of quinoid site of PANI [65]. Some other researchers assigned the peak at +500 mV to the crosslinking of PANI and formation of head to tail dimer [66]. Figure (4) shows the CVs of GC/PANI and GC/CCG/PANI in 0.5 M H$_2$SO$_4$ from -200 to +1000 mV at scan rate 50 mV s^{-1}.
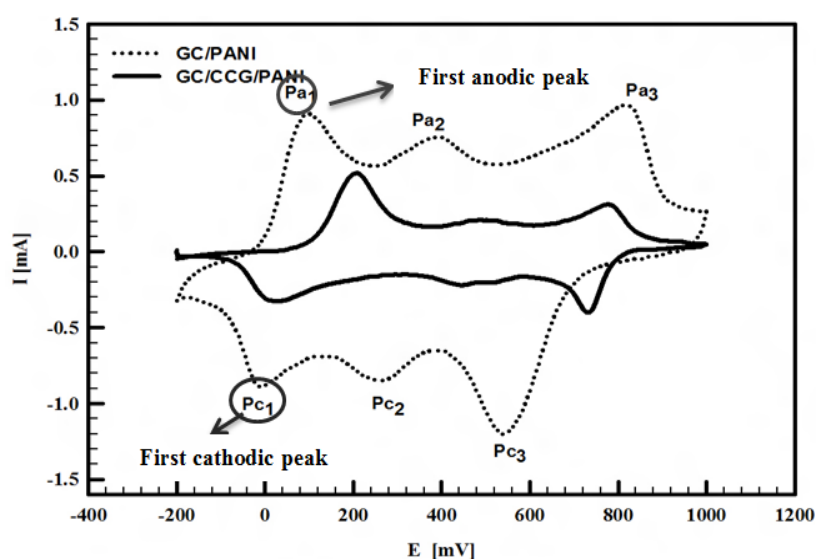
Figure 4. The CVs of GC/PANI (solid line) and GC/CCG/PANI (dotted line) in 0.5 M H$_2$SO$_4$ from -200 to +1000 mV at SR 50 mV s^{-1}.

Comparing between the CVs of GC/PANI and GC/CCG/PANI it is found that both anodic and cathodic peak currents increase sharply in case of GC/CCG/PANI which proves that graphene improves the electron transfer rate for PANI formed onto CCG. Moreover, the double layer capacitance of GC/CCG/PANI is much higher than in case of GC/PANI which indicates that GC/CCG/PANI has much higher electrochemical active area.

It is important to mention that, the number of active sites within the porous polymer layer varies considerably, and is not related to neither the film thickness nor to the real surface area, therefore currents are reported in the data presented in this work rather than current densities.

3.2.3. Effect of polymerization potential of aniline on CCG

In order to assign the best polymerization potential that provides higher electroactivity, aniline was polymerized on GC/CCG at different polymerization potential from +800 to +1100 mV and the formed CCG/PANI film was tested in monomer free solution. The CVs of GC/CCG/PANI (prepared at different polymerization potential) in 0.5 M H_2SO_4 as well as the effect of polymerization potential on 1st peak current is shown on supplementary figure (S (1)). The results indicate that, the best polymerization potential of aniline is +900 mV that yields a relatively higher current of the first peak on the surface of CCG.

3.2.4. Effect of polymerization time of aniline on CCG

The thickness of the resulted polymer can be controlled by controlling the polymerization time. Aniline was polymerized on CCG for different times between 20 s and 120 s at constant polymerization potential of +900 mV. For all polymer films, the thickness was estimated from the amount of charge consumed during the electro-polymerization step. Because of the lack of other experimental facilities, it was not possible to verify the estimated thickness of the films using an alternative technique. Therefore, assuming 100% current efficiency during the electrochemical conversion, it is possible to use the following empirical equation to roughly estimate the film thickness of PANI [63]:

$$d = Q.Mw/z.F.A.\rho$$

Where d is the thickness (cm), Q is the charge (C), Mw is the molecular weight of aniline (93.13 g mol^{-1}), z is the number of electron transferred per aniline unite (0.5), F is Faraday's constant (96485 C mol^{-1}), A is the surface area of electrode (0.0706 cm[2]) and ρ is the density (1.02 g cm^{−3}). The polymer film was alternatively formed using constant applied potential, E_{app} = +900 V for 20 s to 120 s. The total charge passed varied from 8.87 mC to 70.25 mC. The film thicknesses were calculated and summarized in S (4) table.

The PANI films that were polymerized on the surface of GC/CCG at various polymerization times were tested in monomer free solution (0.5 M H_2SO_4) using cyclic voltammetry from -200 to

+1000 mV at scan rate 50 mV s^{-1}. The resulted CVs are shown in S (2A). The values of anodic and cathodic peak currents were plotted versus the polymerization time as shown in S (2B) and (2C), respectively. It is worth to mention that, as the polymerization time increases, the anodic and cathodic peak currents related to the three peaks also increase up to 90 s after that they are not affected largely by the extra applied time so, the polymerization time 90 s was selected as the optimum polymerization time of aniline on the surface of CCG.

3.2.5. Effect of dopant

There are two possibilities for chemical doping of poly(aniline): the "redox" oxidative doping and "non-redox" protonic acids doping. Conducting polymers like poly(acetylene), poly(thiophene) or poly(aniline) undergo p- or n-redox doping by a chemical process during which the number of electrons affects polymer chain changes. The protonic acids doping differ from "redox" doping in that the number of electrons assisted with the polymer chain does not change during the doping process and new electronic states are introduced by protonation.

Emeraldine base form of polyaniline can be doped by sufficiently strong protonic acid to give the corresponding emeraldine base. Upon doping process, only proton from protonating acid is transferred and chemically bonded to polymer chain, the rest of the acid molecule can vary in chemical structure, size and shape without change of electronic properties of the polymer chain. The negatively charged ion (dopant or counterion) stays connected to positively charged polyaniline chain via electrostatic interaction. So functionalization of polyaniline with different dopant can induce different additional properties to polyaniline [67].

The supporting electrolyte plays an important role in the growth of conducting polymer [68]. It is interesting to note the great influence of the counterion on the initial stage of the polymer growth is mainly manifested in:

      i-   The charge transferred during the electropolymerization.

      ii-   The intensity and shape of the polymer redox peaks.

      iii-   The diffusion rate of H$^+$ inside the polymer film.

The charge transferred during the polymerization of aniline can provide information about the kinetics of polymerization step. Thus, by applying a constant potential for a certain time the higher charge indicates the larger thickness of the polymer film obtained that refers to higher polymerization rate. The charge transferred during the polymerization of aniline in the presence of various counterions namely, H_3PO_4, HCl, HNO_3 and H_2SO_4 as well as the estimated film thicknesses at 900 mV for 90 s are summarized in Table (1). The results show that H_3PO_4 is a relatively "poor" supporting electrolyte for aniline polymerization on CCG where, it shows lower charge value indicating lower rate of polymerization. On the other hand, H_2SO_4 represents the "best" protonic acid among the acids used for electropolymerization of aniline and provided the highest charge value. Additionally both HCl and HNO_3 provided very comparable results and the film thickness obtained using these acids are very close. Therefore, these protonic acids can be ordered in terms of increasing the rate of polymerization of aniline on CCG surface as: $H_3PO_4 <$ HCl $\approx HNO_3 < H_2SO_4$. Moreover, the size /charge ratio and

non-solvent interactions of the counterions should also greatly affect the doping/undoping process of the resulting polymer.

In order to investigate the effect of dopant on the behavior of polymer film, the polyaniline that is deposited on GC/CCG by electropolymerization in different protonic acids (HCl, HNO_3, H_3PO_4 and H_2SO_4) was tested in 0.5 M of the corresponding acid (used in the electropolymerization step) in a monomer free solution using cyclic voltammetry from -200 to +1000 mV at scan rate 50 mV s^{-1}. The typical CVs are shown in Figure (5A). The results show that the counterion has pronounced effects on the shape of the cyclic voltammogram. In case of using H_2SO_4 and HNO_3, the three redox peaks are well resolved as indicated before but displaying lower peak current intensities in case of using HNO_3 compared to the case of H_2SO_4. However, in case of using HCl the 2nd and 3rd redox peak current intensities diminished and for H_3PO_4 only one redox peak around +500 mV was obtained.
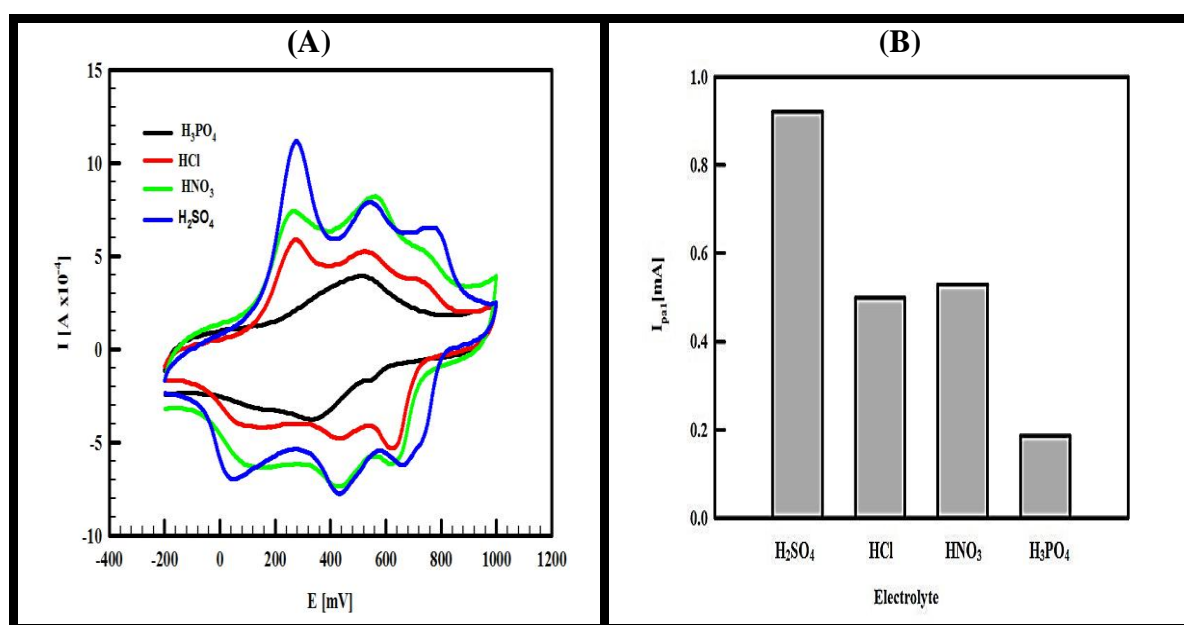

Figure 5. A) The CVs representing the effect of dopant on the electrocatalytic activity of GC/CCG/PANI, H_3PO_4 (black line), HCl (red line), HNO_3 (green line), and H_2SO_4 (blue line), from -200 to 1000 mV at SR 50 mV s^{-1}, the polymerization potential of aniline is +900 mV for 90 s for all dopant and **B)** a histogram between the different used dopant and first anodic peak current recorded in monomer free solution.

Table 1. The total charge passed through the aniline electropolymerization at various polymerization times on GC/CCG as well as the corresponding estimated PANI film thickness.

Dopant (Supporting electrolyte)	Charge [mC]	Estimated Thickness [μm]
H_3PO_4	17.36	4.6
HCl	28.27	7.57
HNO_3	26.37	7.07
H_2SO_4	45.77	12.2

As mentioned before changing the counterion has a large effect on the intensity of redox peaks. From Figure (5A) it is clearly shown that H_2SO_4 provides the highest peak currents among the other protonic acids used in this study while the peak potentials are not largely affected by the type of counterion. The histogram given in Figure (5B) shows the effect of counterion on the value of 1st peak current. The values of peak current and potentials related to the three redox peaks are summarized in table (2).

Table 2. The CV results of GC/CCG/PANI (polymerized in different protonic acids) in 0.5 M H_3PO_4, HCl, HNO_3 and H_2SO_4, the potential window was from -200 to 1000 mV vs. Ag/AgCl electrode at SR 100 mV s^{-1}.

Dopant (Supporting electrolyte)	Ipa (µA)			Epa (mV)			Ipc (µA)			Epc (mV)		
	1st	2nd	3rd	1st	2nd	3rd	1st	2nd	3rd	1st	2nd	3rd
H_3PO_4	---	187	---	---	509	---	---	257	---	---	334	---
HCl	500	79.6	---	274	521	---	90	78	470	68.5	433	621
HNO_3	530	187	---	264	561	---	127	116	476	98.5	417	614
H_2SO_4	920	194	24.4	277	540	757	160	230	580	49	432	657

The effect of dopant on the diffusion of H^+ through the polymer film can be studied by calculating the diffusion coefficient (D) in these protonic acids. Thus, the value of D can be determined by investigating the effect of scan rate on the intensity of the peak current density using Randles Sevcik equation [69] and performing chronoamperometry measurements while taking the real surface area calculated from AFM analysis into consideration. Therefore, the scan rate was varied from 10 to 100 mV.s^{-1} and its influence on the intensity of peak currents was investigated in 0.5 M acid used in the electropolymerization step with a monomer free electrolyte from -200 to 1000 mV (S (3)) for the PANI films prepared in different dopant, H_3PO_4 (A), HCl (B), HNO_3 (C) and H_2SO_4 (D), respectively. By plotting the first anodic current densities observed for three protonic acids (HCl, HNO_3 and H_2SO_4) versus the square root of the scan rate straight lines were obtained as shown in Figure (6A). The first anodic oxidation peak was attributable to radical cations at the N-position which depends on H^+ doping [70, 71]. From these results we can conclude that, the protonation of PANI chains in all used supporting electrolytes used is controlled by the diffusion of H^+. The values of diffusion coefficients of H^+ calculated from the effect of scan rate on the first peak current are summarized in table (3). The results indicate that the highest diffusion coefficient was obtained for GC/CCG/PANI prepared in H_2SO_4 as supporting electrolyte. It is also known that the counterions will be inserted into the film to neutralize positive charge by H^+ protonation during PANI oxidation. The middle oxidation peak ($\approx$0.50 V vs. Ag/AgCl) represents the doping process of counterions [72, 73]. With regard to these four electrolytes, the doping behaviors of counterions were investigated by plotting the middle anodic peak current (I_{pa2}) versus the potential scan rate. H_3PO_4, HNO_3, and HCl (Figure (6B)) show a good linear relationships which indicate that the doping behavior of these supporting electrolytes are controlled consistently by the surface electron transfer process [74]. For H_2SO_4, plotting the I_{pa2} as a function of scan rate gives straight line during the low scan rate while the data points deviate from linearity at high

scan rate. The results indicate that at a low scan rate the SO_4^{2-} or HSO_4^- doping presents a similar behavior to the other supporting electrolytes. As the scan rate increased, the charge transport through the PANI film is apparently diffusional and obeys Fick's law. Consequently the behavior of the SO_4^{2-} or HSO_4^- passing through the PANI film is dominated by Fickian diffusion kinetics [75]. This can be explained on the basis that under a high driving force, the diffusion rate of anions cannot keep up with that of cations.
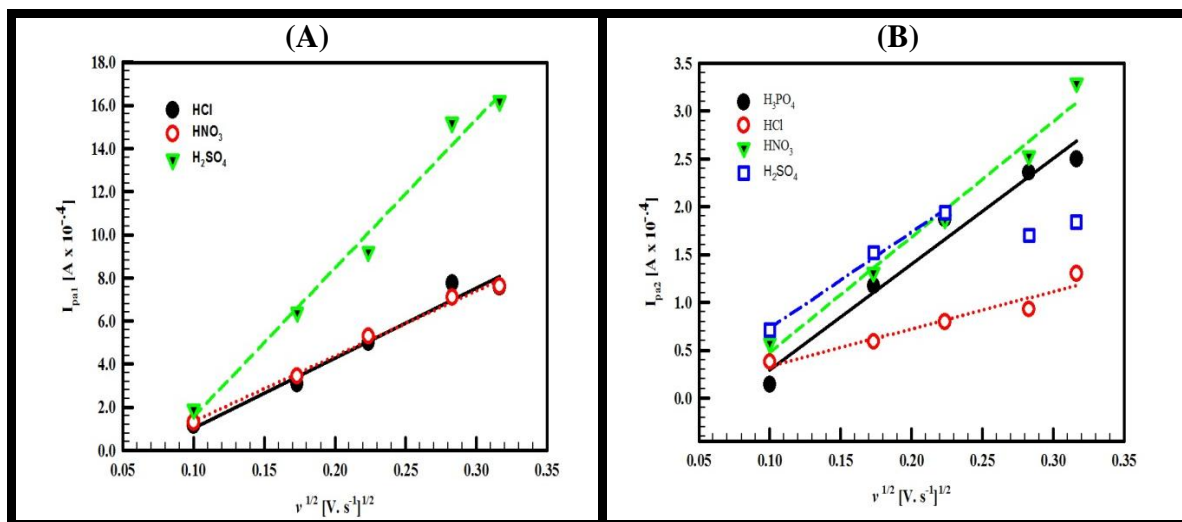

Figure 6. A) A plot of the 1st anodic peak current versus the square root of the scan rate at GC/CCG/PANI in HCl (black line), HNO₃ (red line) and H₂SO₄ (green line) and **B)** A plot of the 2nd anodic peak current versus the square root of the scan rate at GC/CCG/PANI in H₃PO₄ (black line), HCl (red line), HNO₃ (green line) and H₂SO₄ (blue line).

Table 3. The values of D_{H+}, D_C as well as D calculated from the effect of scan rate on the 1st, 2nd peak current and CA of GC/CCG/PANI in 0.5 M H₃PO₄, HCl, HNO₃ and H₂SO₄.

Dopant (Supporting electrolyte)	Scan Rate*		Chronoammperometry*	
	D_{H+}^a [cm² s⁻¹]	D_c^b [cm² s⁻¹]	D_A^c [cm² s⁻¹]	D_{ct}^d [cm² s⁻¹]
H₃PO₄	---	1.550×10^{-7}	5.48×10^{-7}	6.08×10^{-7}
HCl	1.350×10^{-6}	0.193×10^{-7}	9.04×10^{-7}	1.05×10^{-6}
HNO₃	1.160×10^{-6}	1.840×10^{-7}	4.43×10^{-7}	5.85×10^{-7}
H₂SO₄	6.034×10^{-6}	1.270×10^{-7}	3.47×10^{-6}	5.14×10^{-6}

*The technique used for calculation of (D).

[a]Diffusion coefficient of H^+

[b]Diffusion Coefficient of counterion

[c]Diffusion coefficient for anodic scan and

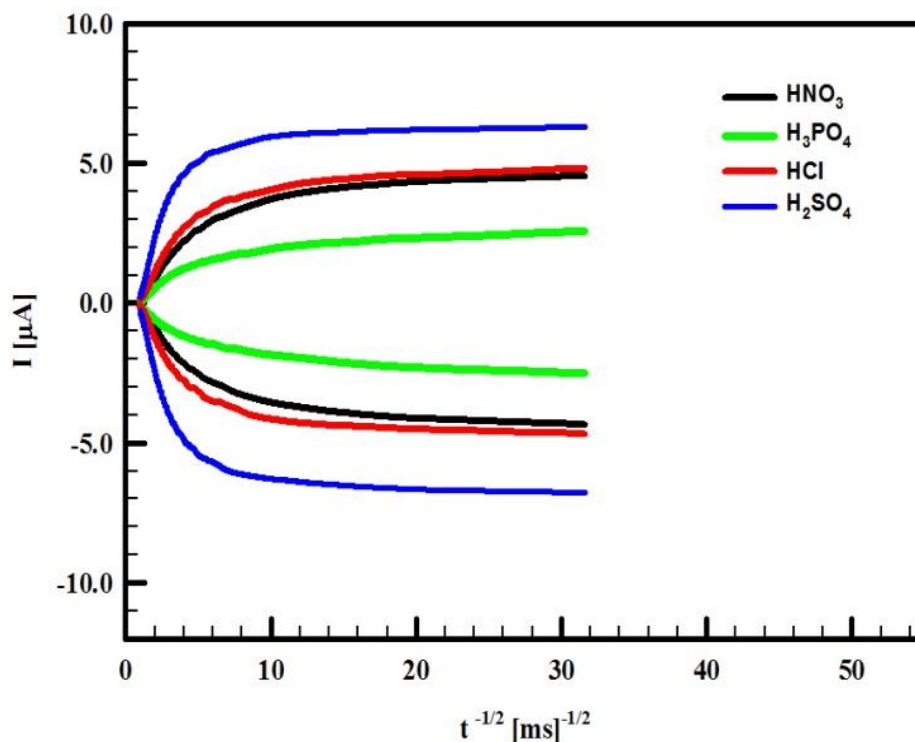[d]Diffusion coefficient for cathodic scan calculated from CA.

Figure 7. The typical CA of GC/CCG/PANI in H_3PO_4 (black line), HCl (red line), HNO_3 (green line) and H_2SO_4 (blue line), the polymerization potential of aniline is +900 mV for 90s for all dopant.

As a result, the redox process is governed by the diffusion of counterions inside the film [75]. The diffusion coefficients of the counterions can be calculated from the effect of scan rate on the intensity of the second anodic peak. In Table (3), the D values calculated from the second anodic peak for the different supporting electrolytes (taking n=1) are given.

Chronoammperometry (CA) was also used for the determination of D and the typical CA curves for the four different supporting electrolytes are shown in Figure (7). The values of D obtained from CA measurements are the average diffusion coefficients of the cation and anion and they are also summarized in Table (3).

3.2.6. Redox reaction on GC/CCG/PANI

There are several complementary properties between conducting polymers (CPs) and CCGs, especially on electrochemical activity, conductivity and mechanical strength. It is expected that the hybridization of CPs with CCG in a composite structure would be attractive for combining the resulting properties of both components and a synergistic effect results that is manifested in a noticeable increase in electron transfer kinetics and improving the properties of the composites.
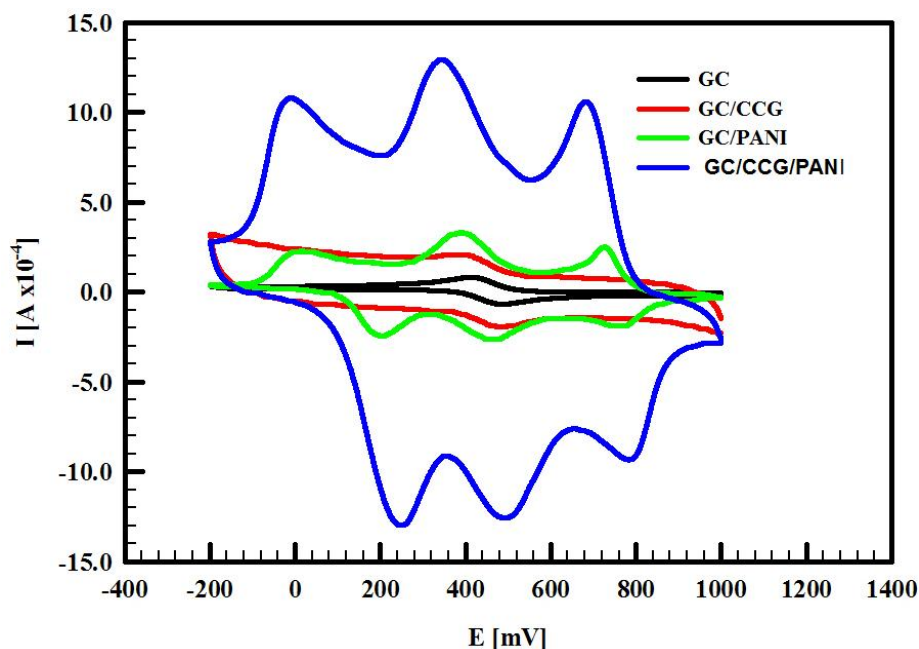
Figure 8. The CV of CG (black line), GC/CCG (red line), GC/PANI (green line), GC/CCG/PANI (blue line) in 6 mM K_3 [Fe (CN)$_6$] + 0.5 M H_2SO_4 from +1000 to -200 mV at SR 50 mV s^{-1} the polymerization potential of aniline is +900 mV for 90s and in 0.5 M H_2SO_4 as supporting electrolyte.

The synergistic effect between CCG and PANI was investigated in a simple redox system such as potassium ferricyanide. CVs of GC, GC/PANI, CCG and GC/CCG/PANI in 6.0 mM K_3 [Fe (CN)$_6$] + 0.5 M H_2SO_4 are shown in Figure (8) where, PANI was polymerized on GC or GC/CCG at 900 mV for 90 s.

Table 4. The CV results of GC, GC/CCG, GC/PANI and GC/CCG/PANI in 6 mM K_3[Fe(CN)$_6$] in 0.5M H_2SO_4.

Electrode	Ipa (µA)	Epa (mV)	Ipc (µA)	Epc (mV)
GC	79.6[§]	411[§]	78.0[§]	482[§]
GC/CCG	116.6[§]	386[§]	100.1[§]	481[§]
GC/PANI	268.8, 136.7 and 41.5[*]	202, 458 and 757[*]	71.4, 224 and 260[*]	13, 388 and 726[*]
GC/CCG/PANI	1000.6, 234 and 231[*]	253, 507 and 810[*]	283, 536 and 947[*]	-22, 336 and 695[*]

[*]The values of peak current and potential for 1st, 2nd and 3rd peak, respectively.

[§]The values of peak current and potential for 1st peak only.

The potential window was selected to cover not only the peak related to Fe^{2+}/Fe^{3+} resox system but also the peaks related to the transformation between PANI forms (the middle peak is related to Fe^{2+}/Fe^{3+}). Comparing between CCG, PANI and CCG/PANI we found that both CCG and PANI provided lower peak currents compared to CCG/PANI by one order of magnitude. This result refers to the synergism between PANI and CCG and table (4) contains the peak currents and potentials obtained for the four electrodes, GC, GC/CCG, GC/PANI and GC/CCG/PANI in 6.0 mM K_3 [Fe $(CN)_6$] + 0.5 M H_2SO_4, respectively.

4. CONCLUSION

- Graphene was prepared chemically via microwave method then aniline was electropolymerized on its surface to form CCG/PANI composites which provided higher electrocatalytic activity in monomer free solutions compared to both CCG and PANI.
- Optimization of electropolymerization of PANI on the surface of CCG was achieved by studying the effect of polymerization potential and polymerization time.
- Different protonic acid was used as dopant and supporting electrolyte for aniline polymerization. The results show that H_3PO_4 is a "poor" supporting electrolyte for aniline polymerization while H_2SO_4 provided the higher polymerization charge and higher current acid among the acids used for electropolymerization of aniline on CCG surface. Both HCl and HNO_3 provided very comparable results whether in their polymerization charge or in the values peak currents in monomer free solutions.
- The effect of scan rate in monomer free solutions which contains different supporting electrolytes as well as CA was studied and the diffusion coefficients of H^+ through the polymer layer were calculated. In H_2SO_4, the highest H^+ diffusion coefficient value was obtained.
- The doping behaviors of the counterions were investigated by plotting the middle anodic peak current (I_{pa2}) versus the potential scan rate. H_3PO_4, HNO_3, HCl and H_2SO_4. The results show that in H_3PO_4, HNO_3, and HCl a linear relationship was obtained which indicates that the doping behavior of these supporting electrolytes are controlled consistently by the surface electron transfer process. While in H_2SO_4 different behavior at high scan rate was obtained that shows a Fickian diffusion kinetics.
- CCG/PANI was also investigated in redox system such as potassium ferricyanide and the synergism between CCG and PANI for electron transfer rate is observed.

References

1. W. P. Wanga and C. Y. Pana, *Polymer* 45 (2004) 3987.

2. Y. G. Wang, H. Q. Li and Y. Y. Xia, *Adv. Mater.* 18 (2006) 2619.
3. D. W. Wang, F. Li, J. P. Zhao, W. C. Ren, Z. G. Chen, J. Tan, Z. S. Wu, I. Gentle, G. Q. Lu and H. M. Cheng, *ACS Nano* 3 (2009) 1745.
4. A.V. Murugan, T. Muraliganth and A. Manthiram, *Chem. Mater.,* 21 (2009) 5004.
5. J. Yan, T. Wei, B. Shao, Z. J. Fan, W. Z. Qian, M. L. Zhang and F. Wei, *Carbon* 48 (2010) 487.
6. L. L. Zhang, X. S. Zhao and J. S. Wu, *Chem. Mater.* 22 (2010) 1392.
7. Q. Wu, Y. X. Xu, Z. Y. Yao, A. R. Liu and G. Q. Shi, *ACS Nano* 4 (2010) 1963.
8. X. S. Zhou, T. B. Wu, B. J. Hu, G. Y. Yang and B. X. Han, *Chem. Commun.* 46 (2010) 3663.
9. X. B. Yan, J. T. Chen, J. Yang, Q. J. Xue and P. Miele*, ACS Appl. Mater. Interf.* 2 (2010) 2521.
10. L. Al-Mashat, K. Shin, K. K.-Zadeh, J. D. Plessis, S. H. Han, R.W. Kojima, R. B. Kaner, D. Li, X.L. Gou, S. J. Ippolito and W. Wlodarski, *J. Phys. Chem. C* 114 (2010) 16168.
11. Z. X. Wei, M. X. Wan, T. Lin and L. M. Dai, *Adv. Mater.* 15 (2) (2003) 136.
12. S. das Neves and M. A. De Paoli, *Synth. Met.* 96 (1998) 49.
13. H. N. Dinh, J.F. Ding, S.J. Xia and V.I. Birss, *J. Electroanal. Chem.* 459 (1) (1998) 45.
14. C. M. Yang and C.Y. Chen*, Synth. Met.* 153 (1–3) (2005) 133.
15. J. E. Huang, X. H. Li, J.C. Xu and H.L. Li, *Carbon* 41 (14) (2003) 2731.
16. D. J. Guo and H.L. Li, J. *Solid State Electrochem.* 9 (6) (2005) 445.
17. W. Feng, X.D. Bai, Y.Q. Lian, J. Liang, X.G. Wang and K. Yoshino, *Carbon* 41 (8) (2003) 1551.
18. Y. Mao, Y. Bao, S. Gana, F. Li and L. Niu, *Biosensors and Bioelectronics* 28 (2011) 291– 297.
19. O. leenearts, B. Partoens and F. M. Peeters, *Microelectr. J.* 40 (2009) 860.
20. K. S. Novoselov, A. K. Geim, D. Jiang, V. Morozov, Y. Zhang, S. V. Dubonos, I. V. Grigorieva and A. A. Firsov, *Science* 306 (2004) 666.
21. J. H. Chen, M. Ishigami, C. Jang, D. R. Hines, M. S. Fuhre and E. D. *Williams, Adv. Mater.* 19 (2007) 3623.
22. S. Mikhailov (ed.), *Physics and Applications of Graphene- Experiments*, InTech Janeza Trdine, Rijeka, Croatia (2011).
23. J. Wintterling and M.-L. Bocquet, *Surf. Sci.* 603 (2009) 1841.
24. C. J. Pool, *Solid State Commun.* 150 (2010) 632.
25. Y. Li, L. Tang and J. Li, electrochem. *Commun.*11 (2009) 846.
26. Z. P.-Inga, J. S. Murry, M. E. Grice, S. Boyd, C. J. O'Conner and P. Politzer, *J. Mol. Struct. Theochem.* 549 (2001)147.
27. L. Tang, Y. Wang, Y. Li, H. Feng, J. Lu and J. Li, *adv. Funct. Mater* 19 (2009) 2782.
28. L. Dong, R. R. S. Gari, Z. Li, M. M. Craig, S. Hou, *Carbon* 48 (2010) 781.
29. J. Wu, M. Agrawal, H. A. Becerril, Z. Bao, Z. Liu, Y. Chen and P. Peumans, *ACS Nano*, 4 (2010) 43.
30. J-H. Chen, W. G. Cullen, C. Jang C, M. S. Fuhrer and E. D. Williams, Phys. Rev. Lett. 102 (2009) 236805.
31. P. Lian, X. Zhu, S. Liang, Z. Li, W. Yang and H. Wang, *Electrochem. Acta* 55 (2010) 3909.
32. J. Wu, Y. Wang, D. Zhang and B. Hou, *J. Power Sources* 196 (2011) 1141.
33. S. Liu, J. Wang, J. Zeng, J. Ou, Z. Li, X. Liu and S. Yang, *J. Power Sources* 195 (2010) 4628.
34. K. I. Bolotin, K. J. Sikes, Z. Jiang, M. Klima, G. Fudenberg, J. Hone, P. Kim and H. L. Stormer, *Solid State Commun* 146 (2008) 351.
35. R. R. Nair, P. Blake, A. N. Grigorenko, K. S. Novoselov, T. J. Booth, T. Stauber, N. M. R. Peres and A. K. Geim, *Science* 320 (2008) 1308.
36. M. Zheng, K. Takei, B. Hsia, H. fang, X. Zhang, N. Ferralis, H. Ko, Y.-L. Chueh, Y. Zhang, R. Mabudian and A. Javey, *Appl. Phys. Lett*. 96 (2010) 063110.
37. D. Li and R. B. Kaner, *Science*, 320 (2008) 1170.
38. S. Stankovich, D. A. Dikin, G. H. B. Dommett, K. M. Kohlhaas, E. J. Zimney, E. A. Stach, R. D. Piner, S. T. Nguyen and R. S. Ruoff, *Nature* 442 (2006) 282.
39. F. Uddin, Metall. Mater. Trans. A 39 (2008) 2805.

40. Y. Z. Bao, L. F. Cong, Z. M. Huang and Z. X. Weng, *J. Mater. Sci.* 43 (2008) 390.
41. Q. Li, O. K. Park and J. H. Lee, *Adv. Mater. Res.* 79 (2009) 2267.
42. T. Jeevananda, Y. K. Jang, J. H. Lee, Siddaramaiah, M. V. D. Urs and C. Ranganathaiah*, Polym. Int.* 58 (2009) 755.
43. Q. Li, Siddaramaiah, N. H. Kim, G. H. Yoo and J. H. Lee, *Compos. Part B* 40 (2009) 218.
44. B. M. Renukappa, Siddaramaiah, R. D. S. Samuel, J. S. Rajan and J. H. Lee, *J. Mater. Sci. Mater. Electron.* 20 (2009) 648.
45. Q. Li, J. W. Kim, T. H. Shim, Y. K. Jang and J. H. Lee*, Adv. Mater. Res.* 47 (2008) 226.
46. W. Zhang, R. S. Blackburn and A. D.-Sanij, *Scripta. Mater*. 57 (2007) 949.
47. K. Chrissafis, K. M. Paraskevopoulos, S. Y. Stavrev, A. Docoslis, A. Vassilio and D. N. Bikiaris, *Thermochim. Acta* 465 (2007) 6.
48. H. Wang, H. Zhang, W. Zhao, W. Zhang and G. Chen, *Compos. Sci. Technol.* 68 (2008) 238.
49. A. Yu, P. Ramesh, M. E. Itkis, B. Elena and R. C. Haddon., *J. Phys. Chem. C*, 111 (2007) 7565.
50. A. Debelak, K. Lafdi, *Carbon* 45 (2007) 1727.
51. X. Chen, Y. P. Zheng, F. Kang and W. C. Shen, *J. Phys. Chem. Solids* 67 (2006) 1141.
52. S. Ansari and E. P. Giannelis*, J. Polym. Sci. Part B: Polym. Phys.* 47 (2009) 888.
53. T. Ramanathan, A. A. Abdala, S. Stankovich, D. A. Dikin, M. H. Alonso, R. D. Piner, D. H. Adamson, H. C. Schniepp, X. Chen, R. S. Ruoff, S. T. Nguyen, I. A. Aksay, R. K. Prud'Homme and L. C. Brinson, *Nat. Nanotechnol.* 3 (2008) 327.
54. Y. R. Lee, A. V. Raghu, H. M. Jeong and B. K. Kim, *Macromol. Chem. Phys*. 210 (2009) 1247.
55. Y. Xu, Y. Wang, J. Liang, Y. Huang, Y. Ma, X. Wan and Y. Chen, *Nano Res*. 2 (2009) 343.
56. H. Quan, B. Zhang, Q. Zhao, R. K. K. Yuen and R. K. Y. Li, *Compos. Part A*, 40 (2009) 1506.
57. G. Eda and M. Chhowalla, *Nano Lett*. 9 (2009) 814.
58. J. Liang, Y. Xu, Y. Huang, L. Zhang, Y. Wang, Y. Ma, F. Li, T. Guo and Y. Chen, *J. Phys. Chem.* 113 (2009) 9921.
59. H. Wang, Q. Hao, X. Yang, L. Lu and X. Wang, *ACS Applied Mater. Interf.* 2 (2010) 821.
60. W. S. Hummers and R. E. Offeman*, J Am. Chem. Soc.* 80 (1958)1339.
61. H. M. A. Hassan, V. Abdelsayed, A. S. Khder, K. M. AbouZeid, J. Terner, M. Samy El-Shall, S. I. Al-Resayes and A. A. El-Azhary, *J. Mater. Chem.* 19 (2009) 3832.
62. J.-J. Shi, G.-H. Yang and J.-J. Zhu, *J. Mater. Chem.* 21 (2011) 7343.
63. M. H. P.-Azar, B. Habibi, *Electrochim. Acta* 52 (2007) 4222.
64. S. Nakabayashi and A. Kira, *J. Phys. Chem.* 96 (1992) 1021.
65. W.-C. Chen, T.-C. Wen and A. Gopalan., *Synth. Met.* 128 (2002) 179.
66. S. E. Moulton, P. C. Innis, L. A. P. K.-Maguire, O. Ngamna and G. G. Wallace, *Curr. Appl. Phys.* 4 (2004) 402.
67. Z. Zhenga, Y. Dua, Q. Fenga, Z. Wanga and C. Wanga, *J. Mol. Catal. A-Chem*. 80 (2012) 353.
68. M. Sniechowski, Structure and Dynamics of Conduction Polyaniline Based Compounds, PhD thesis, AGH University of Science and Technology, faculty of Physics and Computer Science, Poland, 2005.
69. X.-G. Zhang, Y. Murakami, K. Yahikozawa and Y. Takasu, *Electrochim. Acta*, 42, (1997) 223.
70. A. J. Motheo, J. R. Santos Jr, E. C. Venancio and L. H. C. Mattoso, *Polymer* 39 (1998) 6977.
71. Watanabe, K. Mori, M. Mikuni, Y. Nakamura and M. Matsuda, *Macromolecules* 22 (1989) 3323.
72. Watanabe, K. Mori, Y. Iwasaki, Y. Nakamura and S. Niizuma, *Macromolecules* 20 (1987) 1793.
73. E .M. Genies and M. Lapkowski, *J. Electroanal. Chem.,* 236 (1987) 189.
74. D. Orata and D. A. Buttry, *J. Am. Chem. Soc.* 109 (1987) 3574.
75. W. Pan, X. Chen, M. Guo, Y. Huang and S. Yao, *Talanta* 73 (2007) 651.
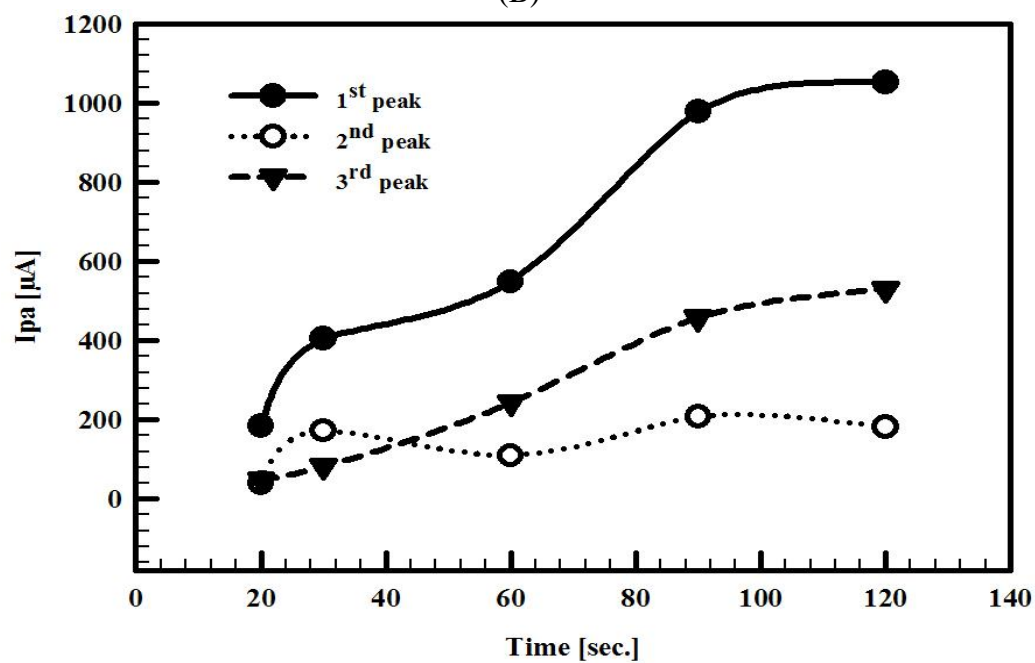
Supplementary Figures and Tables:

(A)

(B)
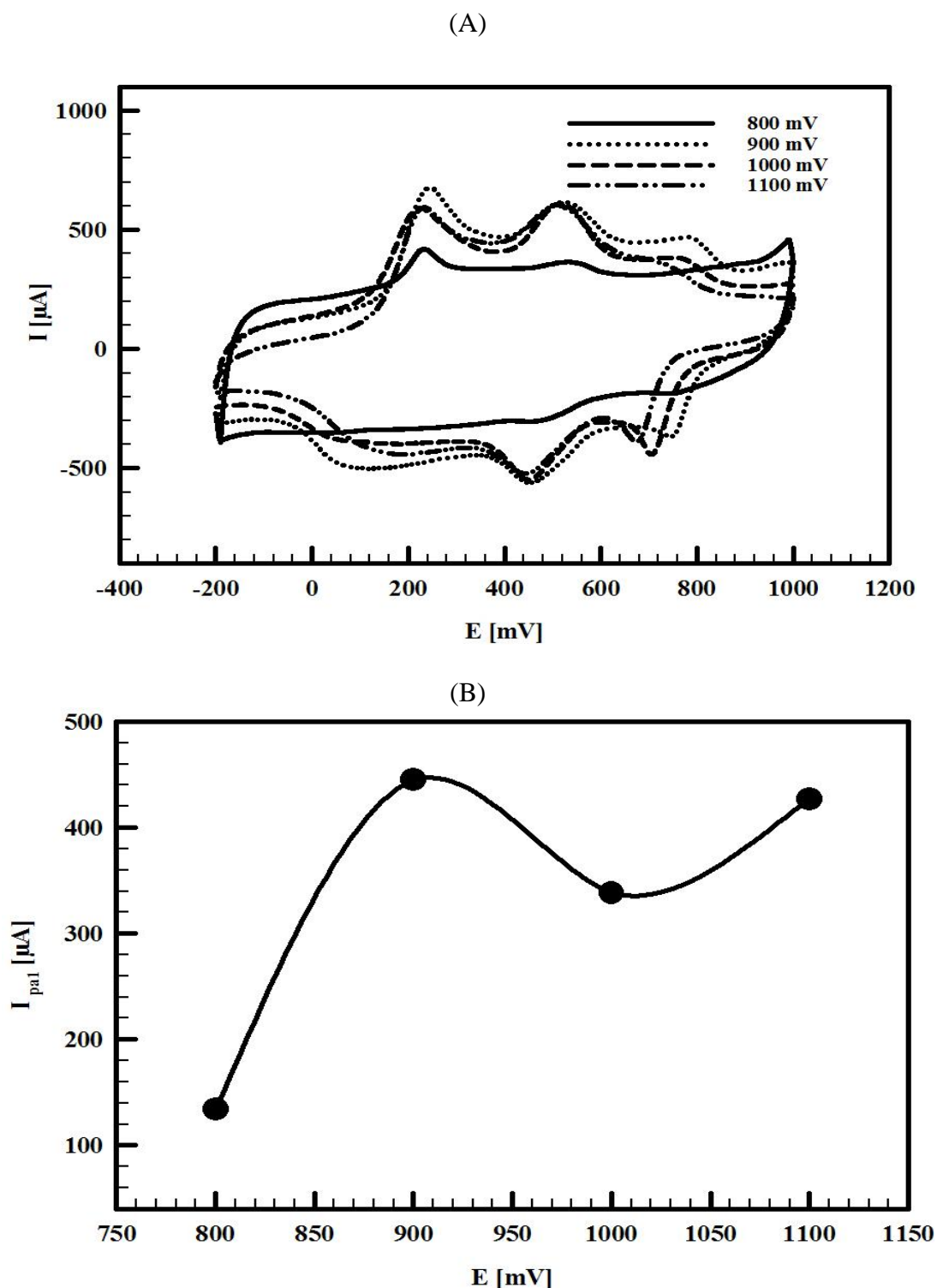
S (1): A) The CVs showing the effect of polymerization potential of aniline on GC/CCG, ——+800, ·····
+900, − − − +1000 and −··− +1100 mV and B) A plot of polymerization potential and first
anodic peak current in 0.5 M H_2SO_4 from -200 to 1000 mV at SR 50 mV s^{-1}.
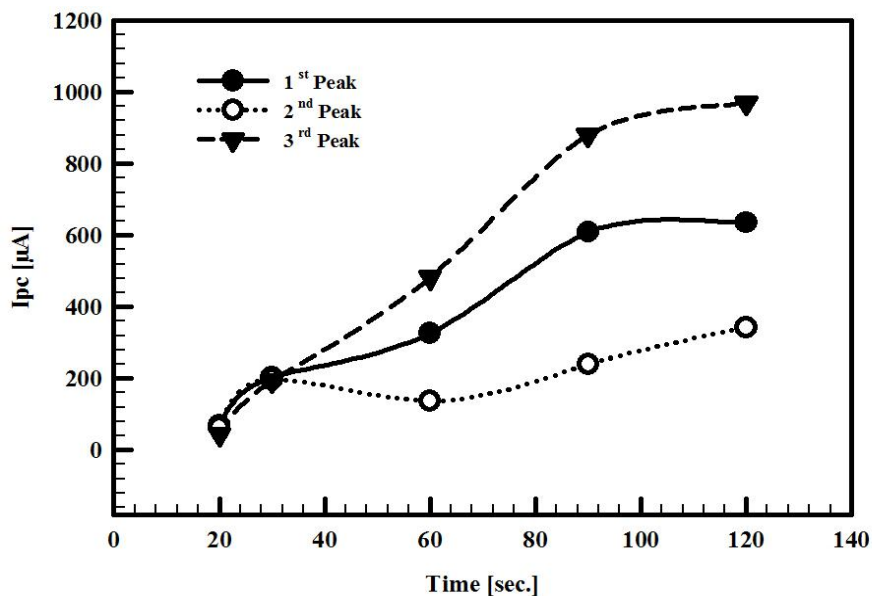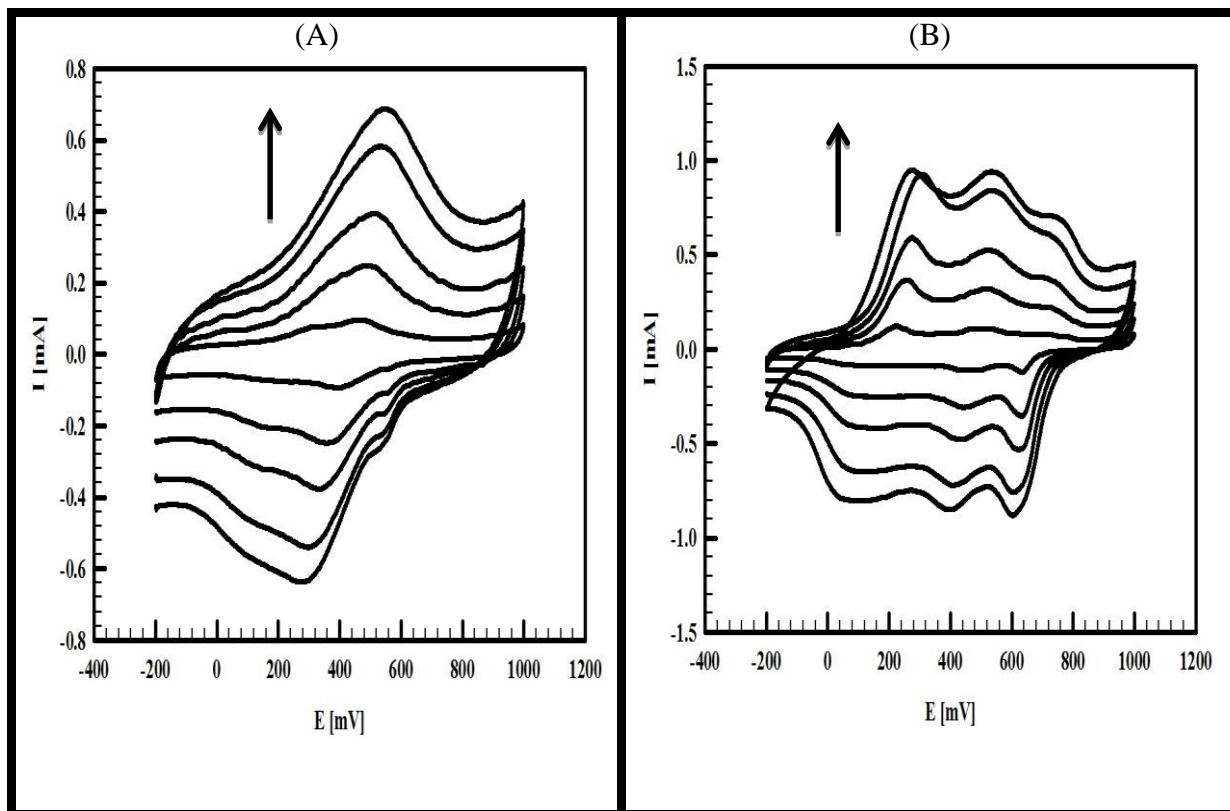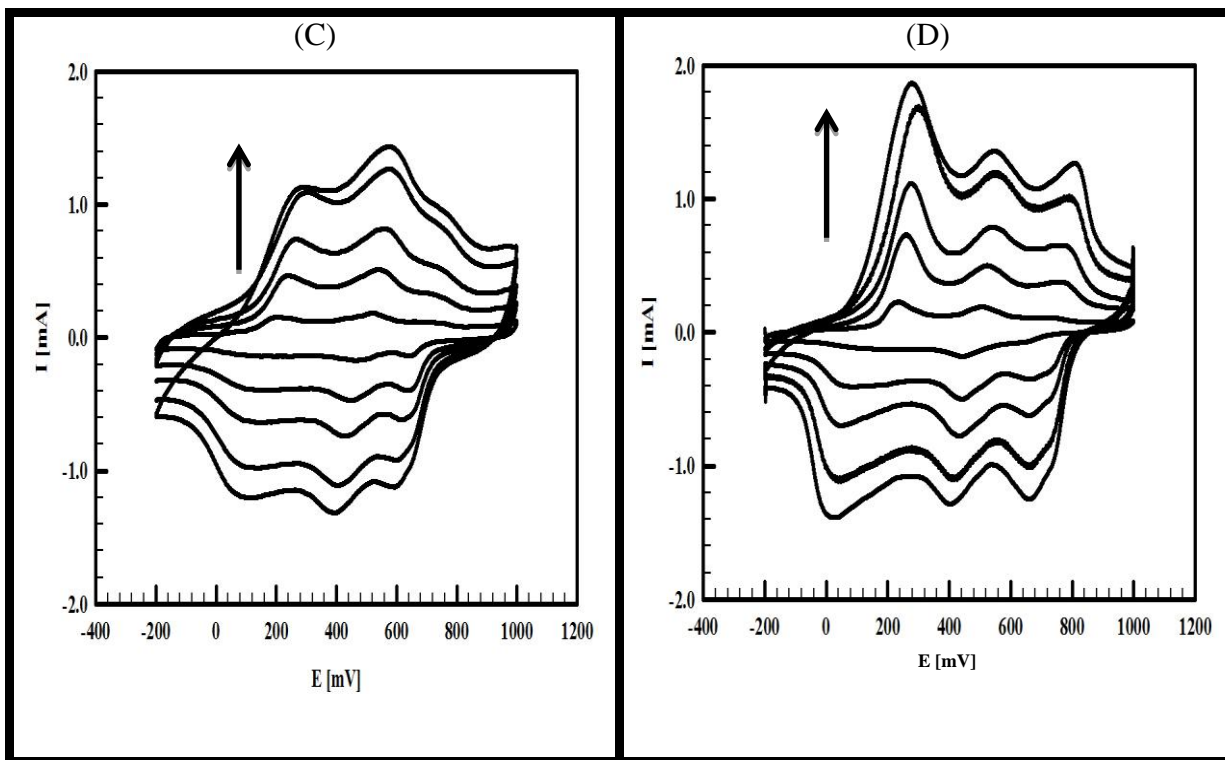
(A)
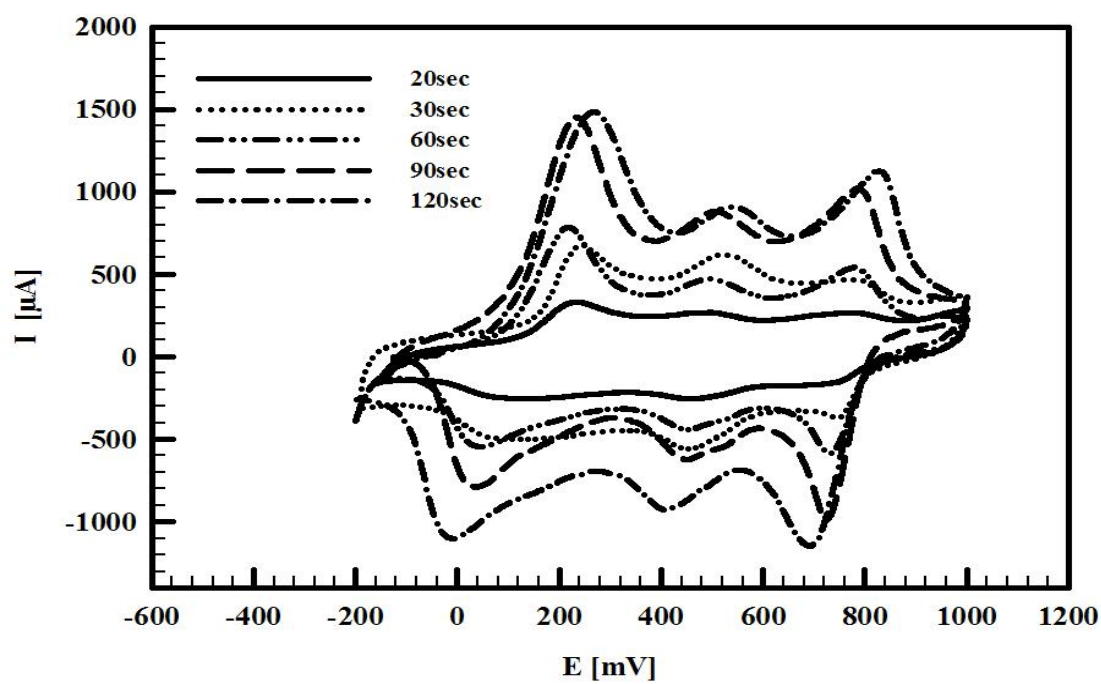
(B)

(C)

S (2): A) The CVs showing the effect of polymerization time of aniline on GC/CCG, ——20s, ····· 30s, – ·· –60s and — — — 90s and – · – · – 120s, B) A plot of polymerization time and 1st (solid line), 2nd (dotted line) and 3rd (dashed line) anodic peak current and C) A plot of polymerization time and 1st (solid line), 2nd (dotted line) and 3rd (dashed line) cathodic peak current in 0.5 M H_2SO_4 from -200 to 1000 mV at SR 50 mV s^{-1}.

S(3). The CVs of GC/CCG/PANI polymerized in A) H_3PO_4, B) HCl, C) HNO_3 and D) H_2SO_4 at various SR (from 10 to100 mV s^{-1}) recorded from -200 to 1000 mV in monomer free solution.

S (4). The total charge passed through the aniline electropolymerization at various polymerization times on GC/CCG as well as the corresponding estimated PANI film thickness.

Polymerization time (s)	Charge (mC)	Estimated thickness (µm)	I_{pa} (µA)			E_{pa} (mV)			I_{pc} (µA)			E_{pc} (mV)		
			1st	2nd	3rd*	1st	2nd	3rd*	1st	2nd	3rd*	1st	2nd	3rd*
20	8.87	2.37	184	39.6	50	233.6	498.5	780	69	63.2	45	100	463.3	741.7
30	17.08	4.57	445.3	172.5	83	245	527	791	204	198	212	68.5	559.5	794
60	23.9	6.4	549	110	243	220	500	783	326	136.8	482	40.3	453	732
90	45.7	12.2	979	208	458	235	510	790	609	240	880	30.7	449	727
120	70.25	18.8	1052	182	531	268.5	543	832	635	343	969	14.7	410	693

*The values of peak current and potentials that observed for 1st, 2nd and 3rd peak in both cathodic and anodic directions.